



Interaction mechanism of okra (*Abelmoschus esculentus* L.) seed protein and flavonoids: Fluorescent and 3D-QSAR studies

Chengyun He^a, Lu Bai^a, Daqun Liu^b, Benguo Liu^{a,*}

^a School of Food Science, Henan Institute of Science and Technology, Xinxiang 453003, China

^b Food Science Institute, Zhejiang Academy of Agricultural Sciences, Hangzhou 310021, China

ARTICLE INFO

Keywords:

Okra seed protein
Flavonoids
3D-QSAR
Interaction
Fluorescence

ABSTRACT

The binding capacity of 10 flavonoids with okra seed protein (OSP) was studied by fluorescence spectroscopy. The structure of flavonoids had an obvious impact on binding performance. The binding ability of flavanone was lower than that of flavone, isoflavone and dihydrochalcone. The binding capacity of flavonoid glycoside was superior to that of the corresponding flavonoid aglycone. The binding ability was positively correlated with the number of phenolic hydroxyl groups on the B ring. The steric field and electrostatic field model constructed by 3D-QSAR method could well explain the above interaction behavior. Thermodynamic analysis suggested that the quenching mechanism of OSP caused by flavonoids was static quenching, and the binding-site number was 1. In addition, hydrogen bonding and van der Waals force dominated this interaction. The 3D and synchronous fluorescence spectra showed that there was no significant change in the polarity of the environment around tryptophan and tyrosine residues during binding.

1. Introduction

Flavonoids are secondary metabolites produced by plants. It widely exists in fruits, vegetables, tea and medicinal materials, and is a widespread phenolic substance in plants (Gülçin, 2012; Gulcin, 2020; Taslimi & Gulçin, 2018). It has many medical benefits, such as anti-cancer (Ahmed et al., 2016; Chae, Xu, Won, Chin, & Yim, 2019), anti-virus (Badshah, Faisal, Muhammad, Poulson, Emwas, & Jaremko, 2021; Cataneo et al., 2021), anti-inflammation (Ozarowski & Karpinski, 2021; Zhang et al., 2011), anti-allergy (Shi, Niu, Zhao, Wang, Jin, & Li, 2018), anti-hypertension (Lv et al., 2013) and anti-diabetes (Lodhi & Kori, 2021). Therefore, the biological activities and corresponding physiological functions of flavonoids have become a research hotspot. But their application is seriously limited because of their low bioavailability and poor stability. Thus, a large number of studies have been carried out to solve these problems of flavonoids. And it is found that some delivery systems based on cyclodextrins, lipids, proteins and emulsions can be used to improve the bioavailability and stability of flavonoids. Liu et al. applied maltosyl- β -cyclodextrin to encapsulate polydatin, and found that it could significantly improve the water solubility and stability of polydatin (Liu, Li, Xiao, Liu, Mo, & Ma, 2015). Wolfram et al. prepared liposomes and loaded hesperidin, which improved the stability and drug

release properties (Wolfram et al., 2016). Yu et al. fabricated the composite colloidal particles of Zein and polysaccharides to stabilize Pickering emulsion of methoxylated flavonoids, and found that the emulsion system enhanced antioxidant activity (Yu, Liu, Wang, Zhang, Jiang, Shan, et al., 2022).

After the interaction of flavonoids with macromolecules, new complexes will be formed, and the concentration, biological activity and spectral properties of the substances will change accordingly. The binding behavior between flavonoids and macromolecules can be studied by fluorescence spectroscopy, and some interaction parameters (binding-site number, binding constant, quenching constant) can be obtained by measuring the changes of parameters before and after the binding. It has been widely used to determine the interaction of whey protein, serum protein, β -casein and lysozyme with flavonoids (Das et al., 2019; Milea et al., 2020). Quantitative Structure-Activity Relationship (QSAR) is often used to explore the relationship between biological activity and molecular structure. 2D-QSAR mainly uses multiple linear regression, principal component analysis and other methods to describe the relationship between physical and chemical properties of molecules and their activities (Boudergua, Alloui, Belaidi, Al Mogren, Ellatif Ibrahim, & Hochlaf, 2019). 3D-QSAR is to establish the relationship between the activity and the 3D structure of molecules based on

* Corresponding author.

E-mail address: liubenguo@hist.edu.cn (B. Liu).

comparative molecular field analysis (CoMFA) and comparative molecular similarity indices analysis (CoMSIA) (Tong, Wu, Bai, & Zhan, 2017). Wu et al. (Wu, Lan, & Jiang, 2015) constructed the CoMFA and CoMSIA models of 22 curcumin derivatives, which indicated that the change of the substituent groups in the corresponding regions could affect the cytotoxicity of MCF-7. Yue et al. combined fluorescence spectroscopy with 3D-QSAR method to explain the binding behavior of Zein and flavonoids (Yue, Geng, Shi, Liang, Wang, & Liu, 2019).

Okra, widely cultivated throughout the world (Balasubramanian & Sadasivam, 1987), is an annual herbaceous plant of the Malvaceae family. Okra is rich in proteins, polysaccharides, flavonoids, vitamins and unsaturated fatty acids, with antioxidant, anti-inflammatory, hypoglycemic and other health functions (Elkhalifa et al., 2021; Esmailzadeh, Razavi, & Hosseinzadeh, 2020; Nikpayam, Safaei, Bahreini, & Saghafi-Asl, 2021). Okra seed protein (OSP) can be used as a supplement to cereal protein and as a carrier to deliver flavonoids (Ofori, Tortoe, & Agbenorhevi, 2020). But so far, there is no systematic report on the interaction between OSP and flavonoids. In view of this, the interaction mechanism of OSP and flavonoids was investigated based on fluorescence spectroscopy and 3D-QSAR methods, so as to provide reference for the application of OSP.

2. Materials and methods

2.1. Materials and chemicals

Okra seeds were provided by Feifan Food Co., LTD (Hebi, China). Flavonoids (taxifolin, rutin, naringin, naringin dihydrochalcone, dihydromyricetin, naringenin, neohesperidin dihydrochalcone, hesperitin, puerarin, phloridzin) were bought from Aladdin (Shanghai, China). All other chemicals were of analytical grade.

2.2. Extraction of OSP

According to the method of Luo et al. (Luo et al., 2022), okra seeds were crushed with a high-speed universal crusher to obtain okra seed powder. The okra seed powder (100 g) was mixed with 1000 mL of *n*-hexane and stirred for 4 h. This operation was repeated until the lipid was completely removed. The defatted okra seed powder was mixed with ultra-pure water at the ratio of 1:20 (w/v), and adjusted pH to 9.0 with 1.0 M NaOH. The mixture was stirred at 25 °C for 2 h, and centrifuged at 8000 × *g* for 20 min. The supernatant was collected and the residue was re-extracted as described above. The supernatant was combined and its pH was adjusted to 4.5 with 1.0 M hydrochloric acid and centrifuged at 6000 × *g* for 15 min. The precipitate was collected, washed 3 times with ultra-pure water, and the pH was adjusted to 7.0. It was re-dissolved in water and dialyzed for 24 h at 4 °C. After vacuum freeze-drying, 9.6 g of okra seed protein was obtained.

2.3. Construction of test system

According to the method of Meng et al. (Meng, Wei, & Xue, 2023), the binding constants of 10 flavonoids with OSP were determined. The OSP sample (0.1 g) was mixed with PBS (pH = 7.0, 10 mM) to form 1 mg/mL stock solution. The flavonoid was dissolved with a small amount of DMSO and diluted with PBS to a solution of 1.25 mM (the final concentration of DMSO was 1 %). The OSP stock solution (5 mL, 1 mg/mL) was mixed with the flavonoid solution of 0, 100, 200, 300, 400, and 500 μL (1.25 mM), and diluted to 25 mL with PBS. The reaction system was stored at 30 °C for 30 min.

2.4. Determination of binding constants

The reaction system obtained in section 2.3 was analyzed by an Agilent Cary Eclipse fluorescence spectrophotometer (Santa Clara, CA). Under the excitation wavelength of 280 nm, the fluorescence emission

spectrum of 300–450 nm was recorded with the voltage of 680 kV. The excitation and emission slits were fixed to 5 nm. In order to eliminate the interference of fluorescence internal filtration effect, the fluorescence data was corrected according to Eq. (1).

$$F = F_{obs} \times e^{\frac{(OD_{ex} + OD_{em})}{2}} \quad (1)$$

Where F_{obs} and F were the fluorescence intensity values before and after calibration. OD_{ex} and OD_{em} were the UV absorbance values of the mixture at the excitation wavelength and emission wavelength, respectively.

Stern-Volmer equation (Eq. (2)) was used to determine the fluorescence quenching mechanism.

$$\frac{F_0}{F} = 1 + K_{SV} \cdot [Q] = 1 + K_q \cdot \tau_0 \cdot [Q] \quad (2)$$

Where, F and F_0 were the fluorescence intensity values of OSP solution with/without flavonoids, respectively; $[Q]$ was the flavonoid concentration; K_{SV} and K_q were the quenching constant and quenching rate constant, respectively; τ_0 was the average lifetime of protein (10^{-8} s).

The binding-site number (n) and binding constant (K_A) for static quenching could be calculated from the double logarithm curve (Eq. (3)):

$$\lg \left[\frac{F_0 - F}{F} \right] = \lg K_A + n \cdot \lg [Q] \quad (3)$$

2.5. Construction of 3D-QSAR model

The 3D structures of flavonoids used was from PubChem database (<https://pubchem.ncbi.nlm.nih.gov/>). The molecular structure was imported into SYBYL 8.1 software, Powell conjugate gradient method was used in the optimization process, Tripos force field and Gasteiger-Huckel charge was adopted. The maximum iteration coefficient was set to 10000, the calculation gradient was 0.005 kJ/mol. The optimized molecule was cut into two fragments R_1 and R_2 by the Topomer method (Table 1), and the corresponding 3D conformations of the fragments were obtained, which were further adjusted to generate the Topomer model. Then, the steric and electrostatic parameters of the flavonoid were used as independent variables, and the pK_A value, the logarithm of K_A , was used as the response value. The model was fitted by Partial Least Squares (PLS) and cross-validated by Leave-One-Out method (LOO).

2.6. Determination of thermodynamic parameters

OSP was mixed with the flavonoid solution (rutin, dihydromyricetin and phloridzin) in accordance with section 2.3, and stored at 30 °C and 37 °C for 30 min, respectively. The corresponding K_A values were measured based on the fluorescence spectra. The thermodynamic parameters (free energy change, ΔG ; entropy change, ΔS ; enthalpy change, ΔH) were calculated using Eqs. (4) and (5):

$$\ln K_A = -\frac{\Delta H}{RT} + \frac{\Delta S}{R} \quad (4)$$

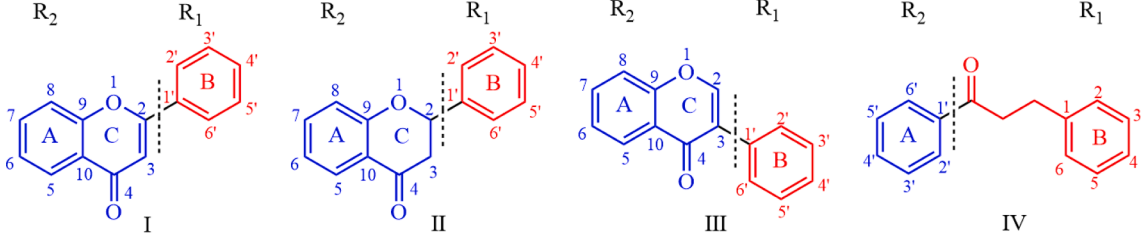
$$\Delta G = \Delta H - T \cdot \Delta S \quad (5)$$

Where R was the gas molar constant ($8.314 \text{ J} \cdot \text{mol}^{-1} \cdot \text{K}^{-1}$), and T was the test temperature.

2.7. Determination of synchronous and 3D fluorescence spectra

OSP was mixed with the flavonoid solution (rutin, dihydromyricetin and phloridzin) in accordance with section 2.3, and kept at 37 °C for 30 min. According to the method of Zhen et al. (Zhen, Geng, Ma, & Liu, 2023), the corresponding synchronous and 3D fluorescence spectra were recorded. The synchronous fluorescence spectra were measured at the excitation wavelength ranges of 250–350 nm ($\Delta\lambda = 15 \text{ nm}$) and

Table 1
Chemical structure and pK_A values of 10 flavonoids.



No	Type	Name	3	4	5	6	7	8	2'	3'	4'	5'	6'	pK _A
1	II	Taxifolin	OH		OH		OH			OH	OH			4.0109
2	I	Rutin	O-		OH		OH			OH	OH			5.2306
			rutinoside											
3	II	Naringin			OH		O-				OH			4.1766
					neohesperidoside									
4	IV	Naringin		OH					OH		O-β-D-		OH	4.8495
											glucopyranoside			
5	II	Dihydromyricetin	OH		OH		OH			OH	OH	OH		4.3304
6	II	Naringenin			OH		OH				OH			4.0770
7	IV	Neohesperidin	OH	OCH ₃					OH		O-		OH	5.1533
					dihydrochalcone						neohesperidose			
8	II	Hesperitin			OH		OH			OH	OCH ₃			4.0978
9	III	Puerarin					OH	C-			OH			4.7875
								glucoside						
10	IV	Phloridzin		OH					O-β-D-		OH		OH	5.2827
									glucopyranoside					

220–350 nm ($\Delta\lambda = 60$ nm), respectively. For 3D fluorescence, the excitation wavelength range was 220–290 nm while the emission wavelength was 290–450 nm. Scanning was performed at a speed of 9600 nm/min. Both the slit widths of emission and excitation were fixed at 5 nm.

2.8. Statistical analysis

The experimental data were analyzed and plotted by Origin 2018 software (Northampton, MA).

3. Results and discussion

3.1. Topomer CoMFA model analysis

The binding constants (K_A) of 10 flavonoids and OSP were determined in this study. According to the structural characteristics of 10 flavonoids, they were divided into four structural types in Table 1, namely flavone (structure I), flavanone (structure II), isoflavone (structure III) and dihydrochalcone (structure IV). According to the difference in pK_A, the following preliminary conclusions could be obtained: (1) The binding ability of flavanone was lower than that of flavone, isoflavone and dihydrochalcone; (2) The binding ability of flavonoid glycoside was higher than that of the corresponding flavonoid aglycone; (3) There was a positive correlation between the binding capacity of the flavonoid aglycone and the number of phenolic hydroxyl groups in the B-ring.

To investigate the effect of the molecular structure of flavonoids on OSP binding, the 3D-QSAR model was established by using the Topomer CoMFA method, which not only inherits the advantages of CoMFA, but also has faster model generation speed. The molecular structure of flavonoids was cut into R₁ and R₂ fragments, and the steric and electrostatic parameters of each fragment were calculated. The PLS regression method could combine the pK_A values with the obtained molecular field energy to construct the 3D-QSAR model. The optimal principal component of the model was 2, and the multiple correlation coefficients of fitting and cross validation were $r^2 = 0.957$ and $q^2 = 0.634$, respectively. The linear regression diagram of the predicted and actual pK_A values of the model for 10 flavonoids is shown in Fig. S1. The data points

were uniformly distributed around the 45° line, confirming a good fitting ability of the model.

3.2. 3D-QSAR analysis

In this study, naringenin (No.6) with the simplest chemical structure was selected as a reference for 3D-QSAR analysis. Fig. 1A and C are the 3D steric field maps of R₁ and R₂, and Fig. 1B and D are the 3D electrostatic field of R₁ and R₂, respectively. In Fig. 1A and C, a large number of green regions were gathered in the positions of C3', C4', C5' of R₁ and C3, C4, C7 and C8 of R₂, indicating that if a bulky substituent group was

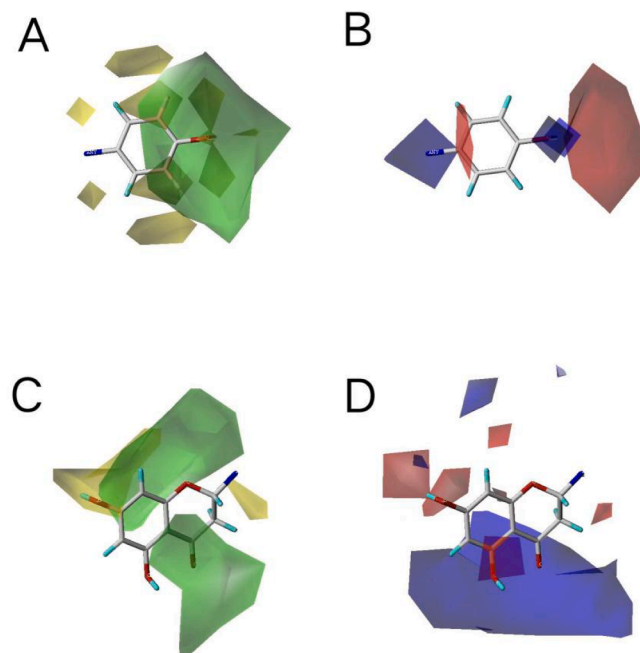


Fig. 1. 3D contour plots of the Topomer CoMFA model. (A: steric field map of R₁-group; B: electrostatic field map of R₁-group; C: steric field map of R₂-group; D: electrostatic field map of R₂-group.).

introduced here, the corresponding flavonoid would have a higher binding capacity. Thus, the H at the C3 position of rutin (No.2) was replaced by O-rutinoside, and the binding ability of rutin was superior to that of taxifolin (No.1). Naringin (No.3) with O-neohesperidoside group at C7 had higher binding ability than naringenin (No.6). On the contrary, there were a large number of yellow regions in the C2' and C6' positions of R₁, which suggested that if large groups were present in these regions, the binding ability of the flavonoid would be reduced. The C3', C4', C5' of R₁ and the C3, C5, C7 positions of R₂ were surrounded the red regions (Fig. 1B and D), which meant that the introduction of negatively charged substituents in these regions could enhance the binding capacity of the corresponding derivatives. For example, the binding capacity of dihydromyricetin (No.5) with -OH at C5' was higher than that of taxifolin (No.1). In Fig. 1D, there were blue regions around C4, C5 and C6 of R₂. If the H at the corresponding site was replaced by a positively charged group, the binding capacity of the derivative could be enhanced.

In addition, 3D-QSAR also confirmed that the binding performance of flavone, isoflavone and dihydrochalcone with OSP was higher than that of flavanone. This may be due to the fact that the B ring of flavones and isoflavone could form the π -conjugated system with its A and C rings, which improved the planar properties of the derivatives. This helped flavonoids bind to the active site of OSP and improved its binding capacity (Geng, Jiang, Ma, Wang, Liu, & Liang, 2020; Yue et al., 2019). The B ring of dihydrochalcone was far away from the A ring and easy to freely rotate orientation, which made it easier to bind to proteins, so its binding ability was higher.

3.3. Binding behavior analysis

Most proteins contain tryptophan, tyrosine and phenylalanine residues, and these aromatic amino acid residues have strong endogenous fluorescence, which makes the protein fluorescent (Lang, Gao, Tian, Shu, Sun, & Li, 2019). Fig. 2 exhibits the effects of three representative flavonoids (rutin, dihydromyricetin and phloridzin) on OSP fluorescence spectra. OSP had a fluorescence characteristic absorption peak around 341 nm. Its fluorescence emission peak intensity decreased significantly and regularly with the increase of the flavonoid concentration, indicating that these flavonoids could quench the endogenous fluorescence of OSP. However, there were some differences in the decreasing trend. Rutin caused the most significant decrease in the fluorescence intensity of OSP, followed by phloridzin and dihydromyricetin. It was inferred that the glycoside substituents on the A ring of flavonoids could affect the binding of flavonoids with OSP.

The quenching mechanism is usually divided into dynamic and static quenching (Yue et al., 2019). In Fig. S2, the F_0/F values at different temperatures had a good linear relationship with flavonoid concentration, indicating that the quenching process belonged to single quenching, that is, static or dynamic quenching (Byadagi, Meti, Nandibewoor, & Chimatadar, 2017). The quenching rate constant (K_q) values of 3 flavonoids were significantly higher than the maximum quenching rate constant of diffusion collision (2.0×10^{10} L/mol·s), which confirmed that flavonoids caused static fluorescence quenching of OSP by forming complexes with OSP.

When small molecules interact with proteins, the small molecules involved in binding and unbound molecules in the system are in a state of equilibrium. The binding-site number (n) and binding constants (K_A), which reflect the equilibrium relationship, could be obtained from the double-logarithmic equation. The n and K_A values of 3 flavonoids with OSP were shown in Table 2 and the double logarithmic curve was shown in Fig. S3. The results showed that rutin, dihydromyricetin and phloridzin had strong binding ability to OSP, and the formed complex had good stability. All n values were close to 1, indicating that there was only one binding site for flavonoids interaction with OSP. Yu et al also found that the n value was close to 1 when studying the interaction between 16 flavonoids and Tartary buckwheat protein (Yu, Liang, & Wang, 2022),

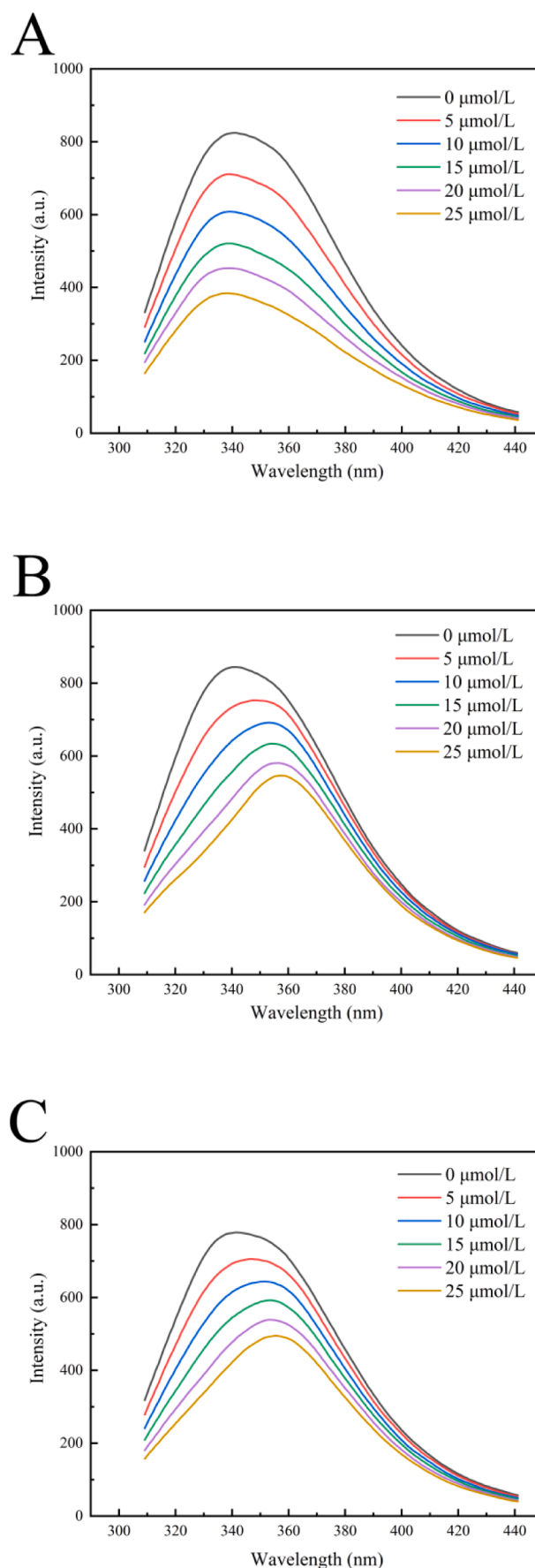


Fig. 2. Effect of flavonoids on the OSP fluorescence spectrum. (A: rutin; B: dihydromyricetin; C: phloridzin).

Table 2

Quenching constants, binding constants and thermodynamic parameters of the 3 flavonoids and OSP.

Flavonoids	T (K)	$10^{12} K_q$ (L·mol ⁻¹ ·s ⁻¹)	pK _A	n	ΔG (KJ·mol ⁻¹)	ΔH (KJ·mol ⁻¹)	ΔS (J·mol ⁻¹ ·K ⁻¹)
Rutin	303	2.2820	5.2306	1.1855	-30.34	-95.45	-214.91
	310	2.0835	4.8590	1.1160	-28.83		
Dihydromyricetin	303	1.5386	4.3304	1.0304	-25.12	-48.19	-76.15
	310	1.8755	4.1428	0.9713	-24.59		
Phloridzin	303	1.3541	5.2827	1.2440	-30.65	-325.37	-972.65
	310	1.3838	4.0161	0.9737	-23.85		

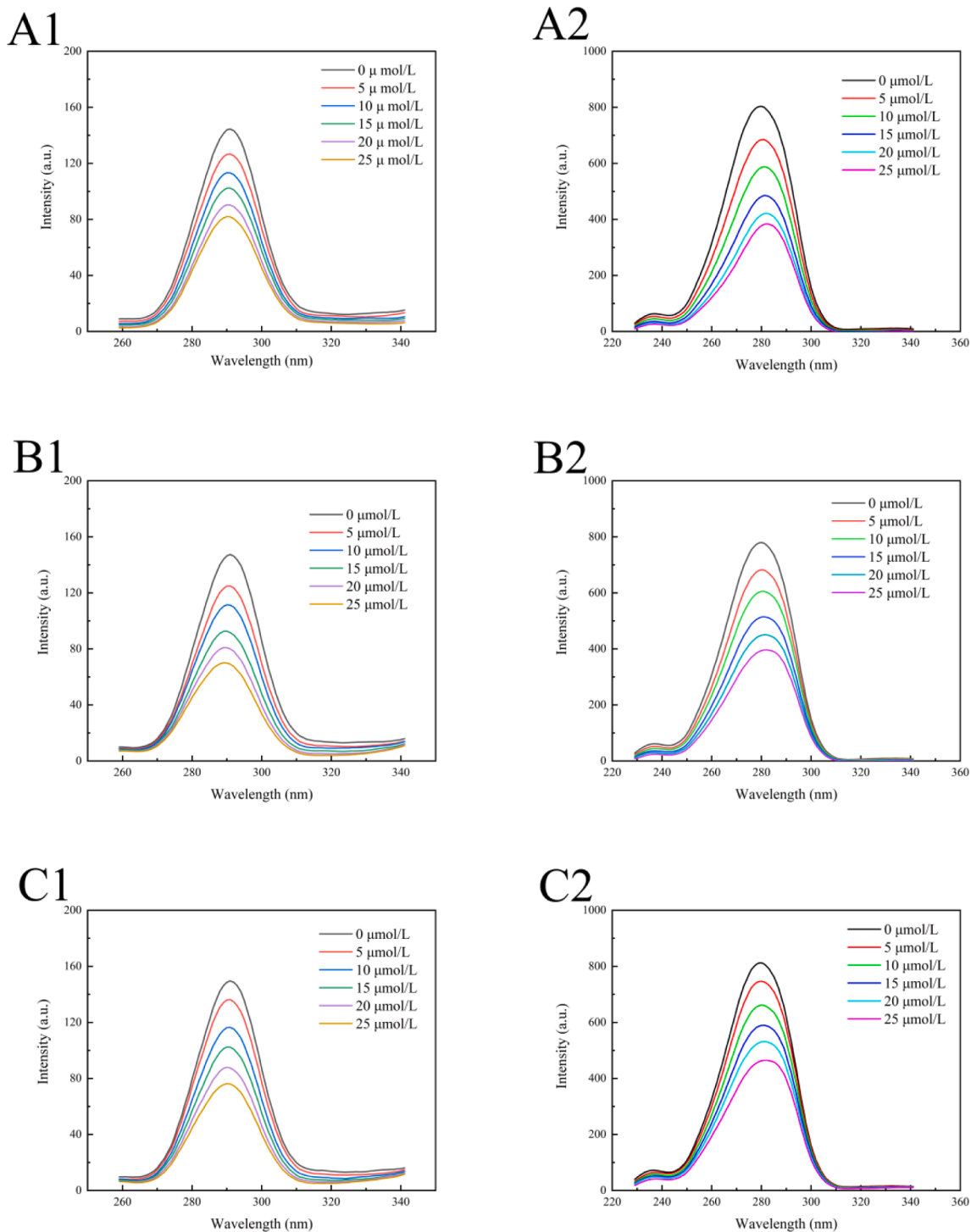


Fig. 3. Effect of the three flavonoids on the synchronous fluorescence spectrum of OSP. (A, B, C are the synchronous fluorescence spectra of rutin, dihydromyricetin, phloridzin at $\Delta\lambda = 15$ nm, respectively; A1, B1, C1 are the synchronous fluorescence spectra of rutin, dihydromyricetin, phloridzin at $\Delta\lambda = 60$ nm, respectively.).

which could be related to the structure of the hydrophobic region on the protein surface. When the temperature increased, the n and K_A values instead decreased, indicating that high temperature was not conducive to the binding of flavonoids to OSP. Zhen et al. found similar experimental results in the study of the binding of dihydromyricetin with α -lactalbumin, suggesting that the increasing temperature promoted the movement of molecules, which was not conducive to the stability of the complex (Zhen et al., 2023; Jiang, Li, Ma, Chen, & Tian, 2020).

3.4. Thermodynamics analysis

Protein molecules and small molecules are combined mainly through non-covalent interactions such as electrostatic interaction, hydrophobic interaction, van der Waals force and hydrogen bonding. Ross et al. summarized the corresponding relationship between the driving force and the thermodynamic parameters based on a large number of experiments: When $\Delta H > 0$, $\Delta S > 0$, the hydrophobic force is the dominant force; When $\Delta H < 0$, $\Delta S < 0$, van der Waals force and hydrogen bonding are the dominant forces; When $\Delta H < 0$, $\Delta S > 0$, the electrostatic force dominates the interaction (Ross & Subramanian, 1980; Jafar et al., 2014). The types of binding between different small organic molecules and proteins are different. According to thermodynamics, at a certain temperature and pressure, whether the bonding of small molecules with protein can proceed spontaneously depends on ΔG of the reaction system. $\Delta G < 0$ is beneficial to the spontaneous reaction.

In Table 2, the ΔS and ΔH of the three flavonoids were all negative, suggesting that van der Waals forces and hydrogen bonding were the dominant forces in the interaction. Rutin, dihydromyricetin and phloridzin had more hydroxyl groups in their structures, making it easier to form hydrogen bonding with OSP. The ΔG of the three flavonoids was all

negative, reflecting that binding was actually a spontaneous process. Therefore, the increasing temperature was not conducive to the binding reaction of flavonoids with OSP. The fluorescence quenching of OSP induced by three kinds of flavonoids was actually an enthalpy driven spontaneous process.

3.5. Synchronous and 3D fluorescence analysis

Synchronous fluorescence spectroscopy is often used as a powerful means to study the effect of small molecules on protein conformation due to its advantages of simplifying spectra and reducing spectral overlap. When $\Delta\lambda = 15$ nm, it only presents the spectral properties of tyrosine residues. When $\Delta\lambda = 60$ nm, it only reflects the fluorescence characteristics of tryptophan residues. Fig. 3 demonstrates the synchronous fluorescence spectra of OSP interacting with 3 flavonoids. The fluorescence intensity of tryptophan and tyrosine residues declined with the increasing flavonoid concentration, but the degree of decrease was different. The tryptophan residue was quenched to a greater extent than the tyrosine residue, so that its binding site was closer to the tryptophan residue. A similar quenching phenomenon had also been reported in the studies about interaction of flavonoids and α -lactalbumin, suggesting that flavonoids bound near the tryptophan residues of the protein (Zhen et al., 2023; Mohammadi & Moeeni, 2015). This is because tyrosine is easily quenched or ionized by quenchers, so the fluorescence information of tryptophan residue in proteins is commonly used to study interaction between biological macromolecules and small organic molecules. Besides, the characteristic peaks of tryptophan and tyrosine residues did not shift, suggesting that the polarity of the environment of these residues did not change significantly.

In order to further analyze the spatial conformation of proteins and

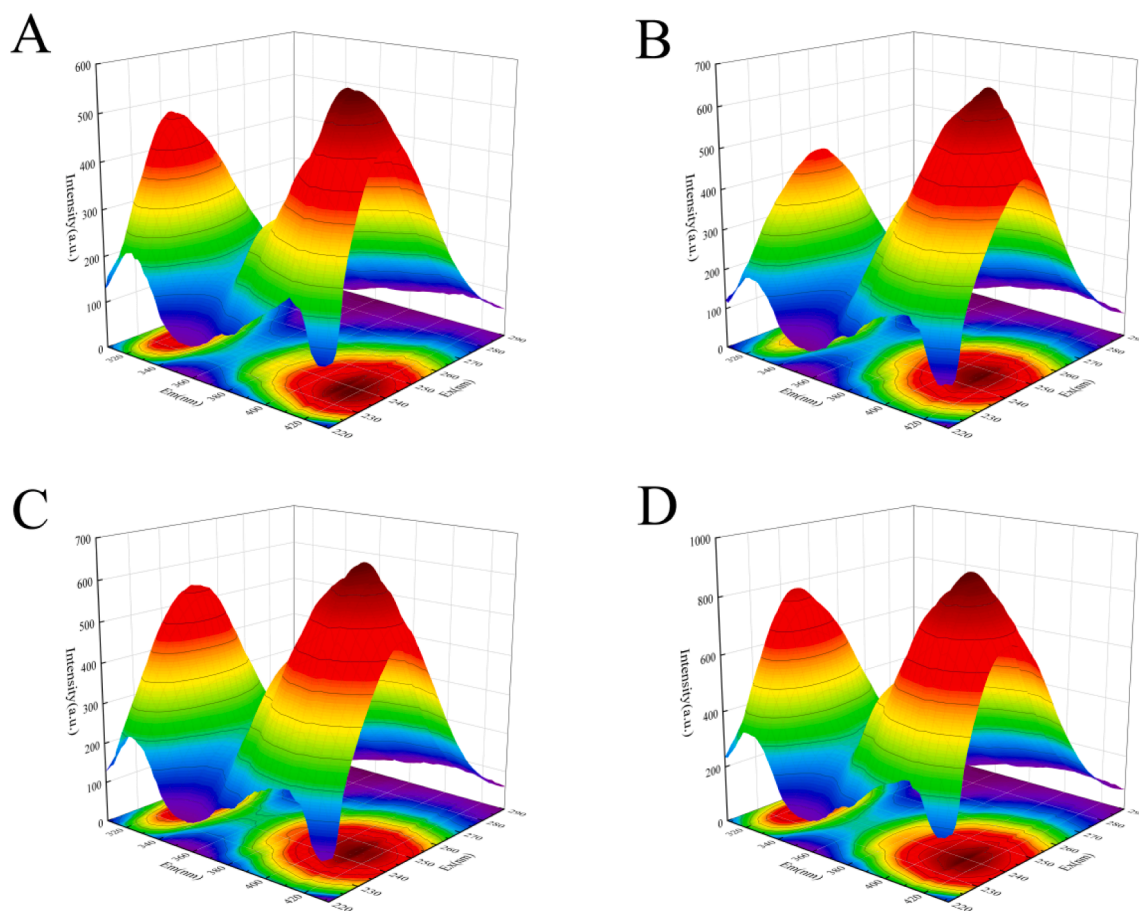


Fig. 4. Effect of flavonoids on 3D fluorescence spectrum of OSP. (A: rutin; B: dihydromyricetin; C: phloridzin; D: OSP without flavonoids.).

the changes in the microenvironment of chromophores, we selected the intermediate concentration of flavonoids (15 μmol) for 3D fluorescence scanning. Fig. 4 showed 3D fluorescence spectra and contour plots with/without of flavonoids. There were two absorption peaks in the 3D fluorescence spectrum of OSP. Peak 1 ($\lambda = 279 \text{ nm}$) exhibited the spectroscopic characteristics of tryptophan residues. Peak 2 ($\lambda = 228 \text{ nm}$) was closely related to the peptide skeleton structure, and its intensity was depend on the secondary structure of protein. The addition of flavonoids reduced the fluorescence intensity of peaks 1 and 2, but the position of the peaks did not change significantly. It could be concluded that the microenvironment of amino acid residues and the secondary structure of proteins did not change significantly during the binding process.

4. Conclusions

Fluorescence spectroscopy was used to study the binding of 10 flavonoids with OSP in this study. The 3D-QSAR model was also established based on the Topomer CoMFA method with pK_A as the modeling response value, which could explain the binding behavior between flavonoids and OSP. It was found that rutin, dihydromyricetin and phloridzin could interact with OSP to quench the intrinsic fluorescence of OSP, and the quenching mechanism was static quenching. There was only one binding site between the three flavonoids and OSP. Van der Waals forces and hydrogen bonding were the dominant forces in the binding process. The microenvironment of tyrosine and tryptophan residues did not change significantly during binding. The obtained results can provide reference for the study of the interaction between flavonoids and proteins, and promote the application of flavonoids and OSP in food.

CRedit authorship contribution statement

Chengyun He: Conceptualization, Methodology, Software, Validation, Formal analysis, Investigation, Data curation, Writing – original draft, Writing – review & editing, Visualization. **Lu Bai:** Methodology, Validation, Formal analysis, Investigation, Data curation, Writing – original draft, Writing – review & editing, Visualization. **Daqun Liu:** Methodology, Validation, Formal analysis, Investigation. **Benguo Liu:** Conceptualization, Methodology, Software, Resources, Writing – original draft, Writing – review & editing, Supervision, Project administration, Funding acquisition.

Declaration of Competing Interest

The authors declare that they have no known competing financial interests or personal relationships that could have appeared to influence the work reported in this paper.

Data availability

Data will be made available on request.

Acknowledgements

This work was supported by the National Natural Science Foundation of China (No. 32072180) and the Natural Science Foundation of Henan Province of China (No. 212300410005). We thank Professor Guizhao Liang of Chongqing University for his support in 3D-QSAR analysis.

Appendix A. Supplementary data

Supplementary data to this article can be found online at <https://doi.org/10.1016/j.fochx.2023.101023>.

References

- Ahmed, S. I., Hayat, M. Q., Tahir, M., Mansoor, Q., Ismail, M., Keck, K., & Bates, R. B. (2016). Pharmacologically active flavonoids from the anticancer, antioxidant and antimicrobial extracts of *Cassia angustifolia* Vahl. *BMC Complementary and Alternative Medicine*, 16, 1–9. <https://doi.org/10.1186/s12906-016-1443-z>
- Badshah, S. L., Faisal, S., Muhammad, A., Poulson, B. G., Emwas, A. H., & Jaremko, M. (2021). Antiviral activities of flavonoids. *Biomedicine & Pharmacotherapy*, 140, Article 111596. <https://doi.org/10.1016/j.biopha.2021.111596>
- Balasubramanian, T., & Sadasivam, S. (1987). Changes in starch, oil, protein and amino acids in developing seeds of okra (*Abelmoschus esculentus* L. Moench). *Plant Foods for Human Nutrition*, 37, 41–46. <https://doi.org/10.1007/BF01092299>
- Boudergua, S., Alloui, M., Belaidi, S., Al Mogren, M. M., Ellatif Ibrahim, U. A. A., & Hochlaf, M. (2019). QSAR modeling and drug-likeness screening for antioxidant activity of benzofuran derivatives. *Journal of Molecular Structure*, 1189, 307–314. <https://doi.org/10.1016/j.molstruc.2019.04.004>
- Byadagi, K., Meti, M., Nandibewoor, S., & Chimatadar, S. (2017). Investigation of binding behaviour of procainamide hydrochloride with human serum albumin using synchronous, 3D fluorescence and circular dichroism. *Journal of Pharmaceutical Analysis*, 7, 103–109. <https://doi.org/10.1016/j.jpha.2016.07.004>
- Cataneo, A. H. D., Avila, E. P., Mendes, L. A. D., de Oliveira, V. G., Ferraz, C. R., de Almeida, M. V., ... Wowk, P. F. (2021). Flavonoids as molecules with anti-Zika virus activity. *Frontiers in Microbiology*, 12, Article 710359. <https://doi.org/10.3389/fmicb.2021.710359>
- Chae, H. S., Xu, R., Won, J. Y., Chin, Y. W., & Yim, H. (2019). Molecular targets of genistein and its related flavonoids to exert anticancer effects. *International Journal of Molecular Sciences*, 20, 2420. <https://doi.org/10.3390/ijms20102420>
- Das, S., Pahari, S., Sarmah, S., Rohman, M. A., Paul, D., Jana, M., & Roy, A. S. (2019). Lysozyme-luteolin binding: Molecular insights into the complexation process and the inhibitory effects of luteolin towards protein modification. *Physical Chemistry Chemical Physics*, 21, 12649–12666. <https://doi.org/10.1039/c9cp01128e>
- Elkhalifa, A. O., Alshammari, E., Adnan, M., Alcantara, J. C., Awadelkareem, A. M., Eltoum, N. E., ... Ashraf, S. A. (2021). Okra (*Abelmoschus Esculentus*) as a potential dietary medicine with nutraceutical importance for sustainable health applications. *Molecules*, 26, 696. <https://doi.org/10.3390/molecules26030696>
- Esmailzadeh, D., Razavi, B. M., & Hosseinzadeh, H. (2020). Effect of *Abelmoschus esculentus* (okra) on metabolic syndrome: A review. *Phytotherapy Research*, 34, 2192–2202. <https://doi.org/10.1002/ptr.6679>
- Geng, S., Jiang, Z. J., Ma, H. J., Wang, Y., Liu, B. G., & Liang, G. Z. (2020). Interaction mechanism of flavonoids and bovine beta-lactoglobulin: Experimental and molecular modelling studies. *Food Chemistry*, 312, Article 126066. <https://doi.org/10.1016/j.foodchem.2019.126066>
- Gülçin, I. (2012). Antioxidant activity of food constituents: An overview. *Archives of Toxicology*, 86, 345–391. <https://doi.org/10.1007/s00204-011-0774-2>
- Gulcin, I. (2020). Antioxidants and antioxidant methods: An updated overview. *Archives of Toxicology*, 94, 651–715. <https://doi.org/10.1007/s00204-020-02689-3>
- Zhen, S. Y., Geng, S., Ma, H. J., & Liu, B. G. (2023). Interaction of α -lactalbumin with dihydromyricetin and its application in nano-emulsion. *International Journal of Food Science & Technology*, 58, 1120–1129. <https://doi.org/10.1111/ijfs.16255>
- Jafar, E. N. D., Panahi-Azar, V., Barzegar, A., Jamali, A. A., Kheiridoosh, F., Kashanian, S., & Omid, Y. J. R. A. (2014). Spectroscopic and molecular modeling studies of human serum albumin interaction with propyl gallate. *RSC Advances*, 4, 64559–64564. <https://doi.org/10.1039/c4ra11103f>
- Jiang, Z., Li, T., Ma, L., Chen, W., Yu, H., Abdul, Q., ... Tian, B. (2020). Comparison of interaction between three similar chalconoids and α -lactalbumin: Impact on structure and functionality of α -lactalbumin. *Food Research International*, 131, Article 109006. <https://doi.org/10.1016/j.foodres.2020.109006>
- Lang, Y. X., Gao, H. Y., Tian, J. L., Shu, C., Sun, R. Y., Li, B., & Meng, X. J. (2019). Protective effects of α -casein or β -casein on the stability and antioxidant capacity of blueberry anthocyanins and their interaction mechanism. *LWT-Food Science and Technology*, 115, Article 108434. <https://doi.org/10.1016/j.lwt.2019.108434>
- Liu, B. G., Li, Y., Xiao, H. Z., Liu, Y. L., Mo, H. Z., Ma, H. J., & Liang, G. Z. (2015). Characterization of the supermolecular structure of polydatin/6-O- α -maltosyl- β -cyclodextrin inclusion complex. *Food Chemistry*, 80, C1156–C1161. doi: 10.1111/1750-3841.12845.
- Lodhi, S., & Kori, M. L. (2021). Structure-activity relationship and therapeutic benefits of flavonoids in the management of diabetes and associated disorders. *Pharmaceutical Chemistry Journal*, 54, 1106–1125. <https://doi.org/10.1007/s11094-021-02329-9>
- Luo, Q. Y., Li, X. M., Zhang, Z. Q., Chen, A. J., Li, S. S., Shen, G. H., ... Hou, X. Y. (2022). Extraction of zanthoxylum seed protein and identification of its simulated digestion products. *LWT-Food Science and Technology*, 161, 11342. <https://doi.org/10.1016/j.lwt.2022.113412>
- Lv, G. Y., Zhang, Y. P., Gao, J. L., Yu, J. J., Lei, J., Zhang, Z. R., ... Chen, S. H. (2013). Combined antihypertensive effect of luteolin and buddleioside enriched extracts in spontaneously hypertensive rats. *Journal of Ethnopharmacology*, 150, 507–513. <https://doi.org/10.1016/j.jep.2013.08.058>
- Meng, Y., Wei, Z. H., & Xue, C. H. (2023). Deciphering the interaction mechanism and binding mode between chickpea protein isolate and flavonoids based on experimental studies and molecular simulation. *Food Chemistry*, 429, Article 136848. <https://doi.org/10.1016/j.foodchem.2023.136848>
- Milea, S. A., Aprodu, L., Mihalcea, L., Enachi, E., Bolea, C. A., Rapeanu, G., ... Stanciuc, N. (2020). Bovine beta-lactoglobulin peptides as novel carriers for flavonoids extracted with supercritical fluids from yellow onion skins. *Journal of Food Science*, 85, 4290–4299. <https://doi.org/10.1111/1750-3841.15513>

- Mohammadi, F., & Moeeni, M. (2015). Analysis of binding interaction of genistein and kaempferol with bovine α -lactalbumin. *Journal of Functional Foods*, *12*, 458–467. <https://doi.org/10.1016/j.jff.2014.12.012>
- Nikpayam, O., Safaei, E., Bahreini, N., & Saghafi-Asl, M. (2021). The effects of okra (*Abelmoschus esculentus* L.) products on glycemic control and lipid profile: A comprehensive systematic review. *Journal of Functional Foods*, *87*, Article 104795. <https://doi.org/10.1016/j.jff.2021.104795>
- Ofori, J., Tortoe, C., & Agbenorhevi, J. K. (2020). Physicochemical and functional properties of dried okra (*Abelmoschus esculentus* L.) seed flour. *Food Science & Nutrition*, *8*, 4291–4296. <https://doi.org/10.1002/fsn3.1725>
- Ozarowski, M., & Karpinski, T. M. (2021). Extracts and flavonoids of *Passiflora* species as promising anti-inflammatory and antioxidant substances. *Current Pharmaceutical Design*, *27*, 2582–2604. <https://doi.org/10.2174/1381612826666200526150113>
- Ross, P. D., & Subramanian, S. (1980). Thermodynamics of macromolecular association reactions: Analysis of forces contributing to stabilization. *Biophysical Journal*, *32*, 79–81. [https://doi.org/10.1016/S0006-3495\(80\)84918-6](https://doi.org/10.1016/S0006-3495(80)84918-6)
- Shi, X. L., Niu, L. Y., Zhao, L. N., Wang, B., Jin, Y. R., & Li, X. W. (2018). The anti-allergic activity of flavonoids extracted from *Citri Reticulatae* Pericarpium. *Journal of Food Processing and Preservation*, *42*, Article e13588. <https://doi.org/10.1111/jfpp.13588>
- Taslimi, P., & Gulçin, I. (2018). Antioxidant and anticholinergic properties of olivetol. *Journal of Food Biochemistry*, *42*, Article e12516. <https://doi.org/10.1111/jfbc.12516>
- Tong, J. B., Wu, Y. J., Bai, M., & Zhan, P. (2017). 3D-QSAR and molecular docking studies on HIV protease inhibitors. *Journal of Molecular Structure*, *1129*, 17–22. <https://doi.org/10.1016/j.molstruc.2016.09.052>
- Wolfram, J., Scott, B., Boom, K., Shen, J. L., Borsoi, C., Suri, K., ... Ferrari, M. (2016). Hesperetin liposomes for cancer therapy. *Current Drug Delivery*, *13*, 711–719. <https://doi.org/10.2174/1567201812666151027142412>
- Wu, Z., Lan, X. B., & Jiang, W. Z. (2015). 3D-QSAR research of curcumin derivatives. *Medicinal Chemistry Research*, *24*, 3460–3466. <https://doi.org/10.1007/s00044-015-1406-9>
- Yu, Y. D., Liang, G. Z., & Wang, H. B. (2022). Interaction mechanism of flavonoids and tartary buckwheat bran protein: A fluorescence spectroscopic and 3D-QSAR study. *Food Research International*, *160*, Article 111669. <https://doi.org/10.1016/j.foodres.2022.111669>
- Yu, Y., Liu, Q., Wang, C., Zhang, D. L., Jiang, B., Shan, Y., ... Ding, S. H. (2022). Zein/pullulan complex colloidal particle-stabilized Pickering emulsions for oral delivery of polymethoxylated flavones: Protection effect and *in vitro* digestion. *Journal of the Science of Food and Agriculture*, *102*, 3952–3963. <https://doi.org/10.1002/jsfa.11742>
- Yue, Y. K., Geng, S., Shi, Y., Liang, G. Z., Wang, J. S., & Liu, B. G. (2019). Interaction mechanism of flavonoids and zein in ethanol-water solution based on 3D-QSAR and spectrofluorimetry. *Food Chemistry*, *276*, 776–781. <https://doi.org/10.1016/j.foodchem.2018.10.083>
- Zhang, L., Ravipati, A. S., Koyyalamudi, S. R., Jeong, S. C., Reddy, N., Smith, P. T., ... Wu, M. J. (2011). Antioxidant and anti-inflammatory activities of selected medicinal plants containing phenolic and flavonoid compounds. *Journal of Agricultural and Food Chemistry*, *59*, 12361–12367. <https://doi.org/10.1021/jf203146e>